

## Supporting Information

# CTAB-assisted synthesis of single-layer MoS<sub>2</sub>/graphene composites as anode materials of Li-ion battery

Zhen Wang,<sup>a</sup> Tao Chen,<sup>a</sup> Weixiang Chen,<sup>\*a</sup> Kun Chang,<sup>a</sup> Lin Ma,<sup>a</sup> Guochuang Huang,<sup>a</sup>  
Dongyun Chen<sup>b</sup> and Jim Yang Lee<sup>b</sup>

*a. Department of Chemistry, Zhejiang University, Hangzhou 310027, P.R. China.*

*b. Department of Chemical and Biomolecular Engineering, National University of Singapore,  
10 Kent Ridge Crescent, 119260, Singapore.*

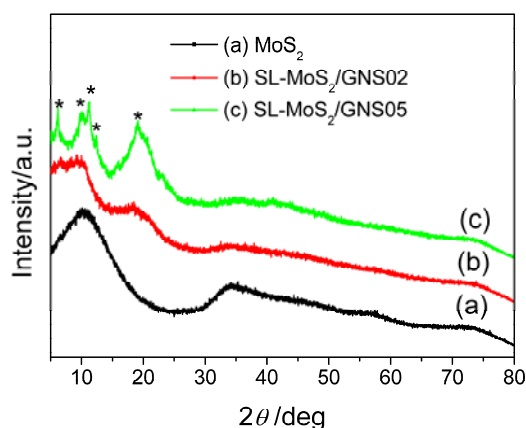


**Fig. S1** XRD patterns of (a) as-prepared MoS<sub>2</sub>, (b) as-prepared SL-MoS<sub>2</sub>/GNS02 and (c) as-prepared SL-MoS<sub>2</sub>/GNS05 composite precursors.

Fig. S1 shows the XRD patterns of the as-prepared MoS<sub>2</sub> and as-prepared SL-MoS<sub>2</sub>/GNS composite precursors before annealing. All the samples hardly reveal the characteristic peaks corresponding to layered MoS<sub>2</sub> crystal. This fact indicates that crystalline of MoS<sub>2</sub> is too poor to reflect its XRD peaks before annealing. As shown in Fig. S1c, the as-prepared SL-MoS<sub>2</sub>/GNS05 composite precursor displays several small and sharp peaks (marked by \*), which are related to being included of surfactant

ion CTA<sup>+</sup> into the composite precursor. The fact agrees with that reported by Bezverkhyy.<sup>1</sup> In order to confirm the reduction of MoS<sub>4</sub><sup>2-</sup> to MoS<sub>2</sub>, the element composition of the as-prepared samples were characterized by EDX. Repeat EDX analysis revealed that the atomic ratio of Mo to S is close to the stoichiometry of MoS<sub>2</sub>, confirming that MoS<sub>4</sub><sup>2-</sup> has been reduced to MoS<sub>2</sub>. It was reported that the strong reduction character of hydrazine can make MoS<sub>4</sub><sup>2-</sup> reduced to MoS<sub>2</sub> during refluxing according the overall reaction:<sup>2</sup>



While GOS was in-situ reduced to GNS by hydrazine solution under refluxing at 95 °C.

MoS<sub>2</sub> and SL-MoS<sub>2</sub>/GNS composites were characterized by TGA as shown in Fig. S2. Fig. S2 shows that MoS<sub>2</sub> starts to lose weight at approximately 430 °C due to the oxidation of MoS<sub>2</sub> to MoO<sub>3</sub>. The SL-MoS<sub>2</sub>/GNS composites exhibit two weight losses. The first one appears at approximately 270 °C, which can probably be attributed to the removal of oxygen-containing groups. The second is only one large continuous weight loss in the range of approximately 365-550 °C. This thermal behavior might be caused by the decomposition of the amorphous carbon and graphene, and oxidation of MoS<sub>2</sub> in the composites. It is very difficult to distinguish the content of graphene from the TGA curves of SL-MoS<sub>2</sub>/GNS composites due to the presence of amorphous carbon. In order to calculate the content of graphene in the SL-MoS<sub>2</sub>/GNS composites, the MoS<sub>2</sub>/GNS (1:2) composite was prepared by the same process without CTAB and characterized by TGA as shown in Fig. S2b. Fig. S2a shows that the pure MoS<sub>2</sub> has an overall weight loss of 91.1%, which well agrees with

the theoretic value (89.9%) of the oxidization reaction of  $\text{MoS}_2$  to  $\text{MoO}_3$ . It was reported that the amorphous carbon and graphene were completely oxidized under  $700^\circ\text{C}$  in air, thus the remaining product of the  $\text{MoS}_2/\text{GNS}$  composites under  $700^\circ\text{C}$  was only  $\text{MoO}_3$ .<sup>3-5</sup> According to Fig. S2b, the content of  $\text{MoS}_2$  in the  $\text{MoS}_2/\text{GNS}$  (1:2) composites was calculated to be about 83.66% and the content of graphene was 16.33%. Because the three composites have the same molar ratio of  $\text{MoS}_2$  to graphene, we can estimate the contents of  $\text{MoS}_2$ , graphene and amorphous carbon in the SL- $\text{MoS}_2/\text{GNS}$  composites and the results are summarized in Table S1. In addition, according the elemental compositions of the samples examined by EDX, we can directly calculate the content of  $\text{MoS}_2$  in the composites (see Table 1), which matches well with the results of the TGA analysis.

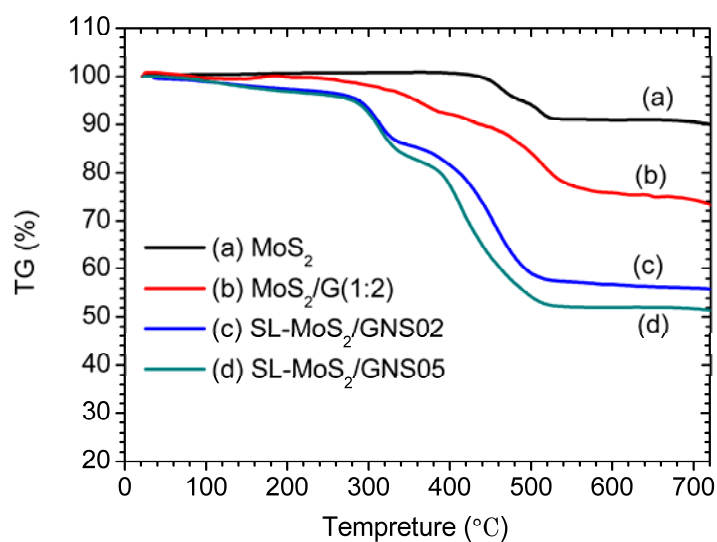


**Fig. S2** TGA curves of (a)  $\text{MoS}_2$ , (b)  $\text{MoS}_2/\text{GNS}$  (1:2), (c) SL- $\text{MoS}_2/\text{GNS02}$  and (d) SL- $\text{MoS}_2/\text{GNS05}$  composites measured at a heating rate of  $10^\circ\text{C min}^{-1}$  in a flowing air.

**Table 1.** The compositions of the samples calculated from the TGA

Samples	MoS <sub>2</sub> /wt%	Graphene /wt%	Amorphous carbon /wt%
MoS <sub>2</sub>	100	—	—
MoS <sub>2</sub> /GNS(1:2)	83.66	16.33	—
SL-MoS <sub>2</sub> /GNS02	63.12	12.32	24.56
SL-MoS <sub>2</sub> /GNS05	56.94	11.12	31.94

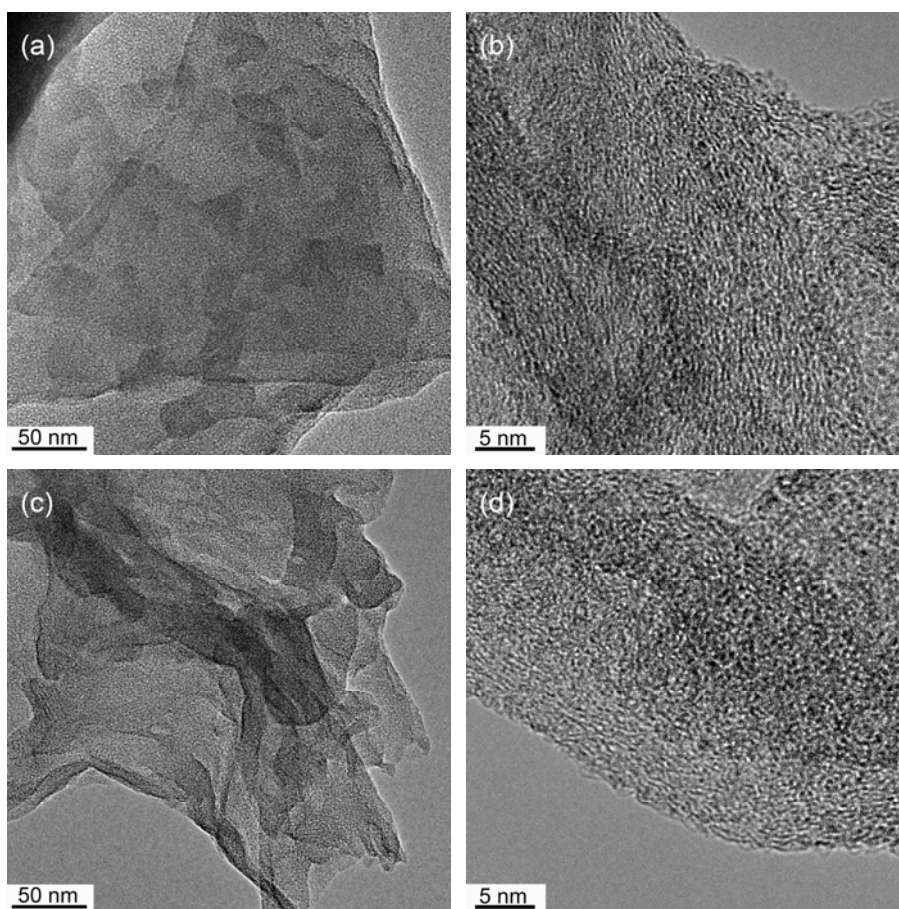


**Fig. S3** TEM and HRTEM images of (a, b) as-prepared SL-MoS<sub>2</sub>/GNS02 and (c, d) as-prepared SL-MoS<sub>2</sub>/GNS05 composites.

The TEM and HRTEM images of the SL-MoS<sub>2</sub>/GNS products before heat-treatment were carried out as shown in Fig. S3. From the HRTEM images, it can be seen that the very short MoS<sub>2</sub> fringes with poor-crystalline are highly dispersed in the composites. Due to the very short fringes and extremely poor-crystalline of MoS<sub>2</sub>,

the XRD patterns of the as-prepared SL-MoS<sub>2</sub>/GNS composite precursors before heat treatment hardly display the characteristic peaks of MoS<sub>2</sub> crystal as shown in Fig. S1.

## References

1. I. Bezverkhyy, P. Afanasiev and M. Lacroix, *Materials Research Bulletin*, 2002, **37**, 161-168.
2. P. Afanasiev, G.-F. Xia, G. Berhault, B. Jouguet and M. Lacroix, *Chemistry of Materials*, 1999, **11**, 3216-3219.
3. S. J. Ding, J. S. Chen and X. W. Lou, *Chemistry-a European Journal*, 2011, **17**, 13142-13145.
4. G. Wang, J. Yang, J. Park, X. Gou, B. Wang, H. Liu and J. Yao, *The Journal of Physical Chemistry C*, 2008, **112**, 8192-8195.
5. C. F. Zhang, Z. Y. Wang, Z. P. Guo and X. W. Lou, *ACS Appl. Mater. Interfaces*, 2012, **4**, 3765-3768.